Formation of an amorphous phase in $Cr_{1-x}Fe_x$ films obtained by thermal evaporation

S. K. Xia and E. Baggio-Saitovitch
Centro Brasileiro de Pesquisas Fisicas, Rua Dr. Xavier Sigaud 150, 22290, Rio de Janeiro, Rio de Janeiro, Brazil

C. Larica
Departamento de Fisica e Quimica, Universidade Federal do Espirito Santo, 29069, Vitoria, Espirito Santo, Brazil
(Received 24 May 1993)

$Cr_{1-x}Fe_x$ alloy films ($\cong$3000 Å) were prepared by thermal coevaporation at room temperature at a deposition rate of 25 Å/min. It was found that a pure amorphous phase can be obtained in the composition range $0.25 < x < 0.60$, while out of this range the bcc crystalline phase appears. The structural characterization and the magnetic properties were studied by x-ray diffraction and Mössbauer spectroscopy, respectively. The crystallization temperature for an amorphous $Cr_{70}Fe_{30}$ film was found to be about 630 K as determined by *in situ* Mössbauer measurements. Since Cr-Fe is not a ready-glass-forming system, the amorphization process was discussed through the thermodynamics of the system and the kinetics of the condensation process.

I. INTRODUCTION

The glass-forming ability (GFA) of an alloy system is influenced by the thermodynamics of the system and the kinetics of the process of phase transformation. The former requires that the driving force, i.e., the difference in Gibbs free energy between amorphous and crystalline states, should be small enough that, once the system relaxes to an amorphous state, the further crystallization transition can be avoided. The kinetics of amorphization involves an atomic relaxation which results in by-passing the nucleation and growth of the crystalline phases, therefore, it is associated with the method of sample preparation.

For the case of amorphization by melt quenching of a liquid binary alloy, the atomic and ionic radii are taken as an important structural criterion.[1,2] Usually the size difference approaching 15% is necessary for ready-glass formation. This criterion is a simple matter of a hindrance of diffusion kinetics, i.e., a limitation of atomic diffusion during cooling, since a binary alloy with a large difference in atomic size between the constituents usually possesses a large bond strength in the liquid.[3,4] This criterion restricts the amorphization in many systems as in the Cr-Fe one (the bond lengths for Cr and Fe pure metals with bcc structure are 0.249 80 and 0.248 23 nm, respectively[5]). However, in an earlier work,[6] we found that a Cr-Fe amorphous phase can be formed by mechanical milling (MM) of a Cr-Fe crystalline alloy. Obviously, amorphization by MM results from different kinetic condition during the phase transformation as compared with the melt-quenching technique.[6,7]

Vapor-quenching techniques such as thermal evaporation and sputtering deposition have been widely used for preparation of amorphous materials because of the very high quenching rate as compared with the melt-quenching method. Sumiyama *et al.*[8-11] have studied a series of film alloys containing Fe and other transition metals and found that amorphous materials can be obtained in the Fe-M systems where M are early transition-metal elements, such as Ti and V. However, for the Cr-Fe system,[11] they only obtained the metastable σ and A_{15} phases. According to them, the reason why amorphous phase could not be formed is the similar atomic size of the two constituents.

In this paper, we report on the formation of an amorphous phase in the Cr-Fe system obtained by thermal evaporation, using a very low deposition rate. We will interpret that such a deposition condition provides a favorable condensation kinetics for amorphization. It will be also shown that the variation in composition, which changes the thermodynamic properties of a system, will affect the GFA. The magnetic properties of the films are also studied.

II. EXPERIMENTAL DETAILS

$Cr_{1-x}Fe_x$ ($0.10 \leq x \leq 1.00$) films were prepared by thermal coevaporation from Cr and Fe pure metals, deposited onto kapton substrates at room temperature (RT). The temperature of the substrate during deposition can be varied up to a maximum value of about 350 K. The vacuum was kept about 3×10^{-7} torr during the depositions. A quartz crystal oscillator was used for both controlling the deposition rate, which was about 25 Å/min for all the films, and monitoring the compositions, which were also determined by energy dispersive analysis (EDS). All the films have a thickness of about 3000 Å.

The structures of the films were determined by x-ray diffraction using Cu-$K\alpha$ radiation performed on a Philips x-ray diffractometer equipped with a LiF monocrhromator. The transmission Mössbauer measurements were performed on all the samples at 4.2 K and RT using a ^{57}Co source in Rh matrix. The velocity scale for the Mössbauer spectra was calibrated related to α-Fe at RT and all the isomer shift values reported here are relative to α-Fe.

In order to study the thermal stability, *in situ*

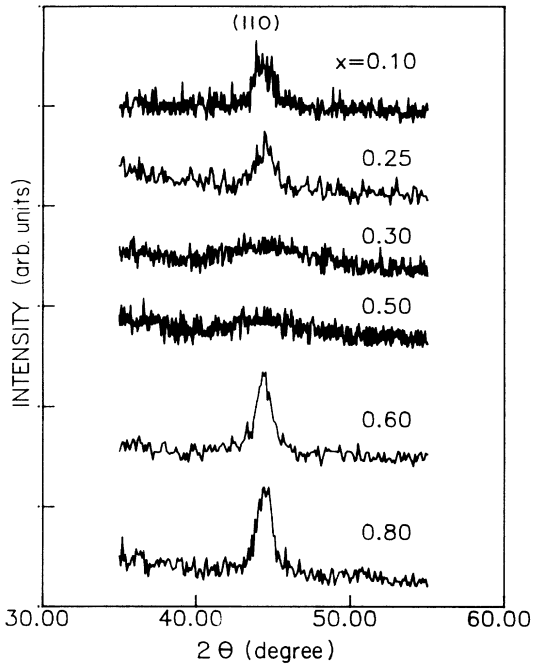

FIG. 1. X-ray-diffraction patterns of the thermal evaporated $Cr_{1-x}Fe_x$ film alloys.

Mössbauer measurements were performed for the $Cr_{70}Fe_{30}$ sample from RT to 823 K in a furnace with a vacuum of about 10^{-4} torr. Before starting each measurement, the sample was kept at the temperature of interest for 30 min, and then the data were accumulated for 30 min.

III. EXPERIMENTAL RESULTS

Figure 1 shows the low-angle x-ray-diffraction patterns for $Cr_{1-x}Fe_x$ films. A halo pattern is prominent for the samples with $0.25 < x < 0.6$, which indicates the formation of an amorphous structure. The bcc structure can be observed for the samples with $x \leq 0.25$ and $x \geq 0.60$. The lattice parameter of the crystalline films decreases with increasing x values as indicated by the shift of the (110) peak to the high angle. The linewidth of this peak is broadened due to the lattice defects and strains retained in the films or to small grain size.

Figure 2 shows the Mössbauer spectra measured at 4.2 K for $Cr_{1-x}Fe_x$ films. The variation of the spectra against composition can be described as follows. With increasing x up to about 0.25, one observes magnetically split spectra similar to the bcc bulk alloys.[12] For $0.25 < x < 0.60$ (which is the region where x-ray diffractions show the halo patterns), the Mössbauer spectra exhibit a broad absorption line. This indicates that the magnetic moment of Fe atoms in the amorphous matrix is strongly reduced. For $0.6 \leq x \leq 0.8$, the spectra are composed of a broad absorption line overlapped with a magnetically split spectrum. This is due to a mixture of amorphous and bcc crystalline phases. Finally, for $x \geq 0.80$, the films exhibit again magnetically split spectra similar to the bulk crystalline alloys,[12] i.e., the bcc crystalline structure is prominent in the materials.

The influence of the composition on the average hyperfine field, $\langle H_{hf} \rangle$, which is approximately proportional to the Fe magnetic moment in the films, is plotted in Fig. 3. The values of $\langle H_{hf} \rangle$ were obtained by fitting the spectra using a hyperfine field distribution (HFD). Since a quadrupole splitting distribution may play an important role in an amorphous material,[6] the fits by using only a HFD for the amorphous films will give an overestimation for the $\langle H_{hf} \rangle$ values. For comparison, the $\langle H_{hf} \rangle$ values for bulk crystalline samples, taken from Ref. 12, are also plotted in Fig. 3. It can be seen that the composition dependence of the crystalline films follows the similar trend as that of bulk samples, while for the

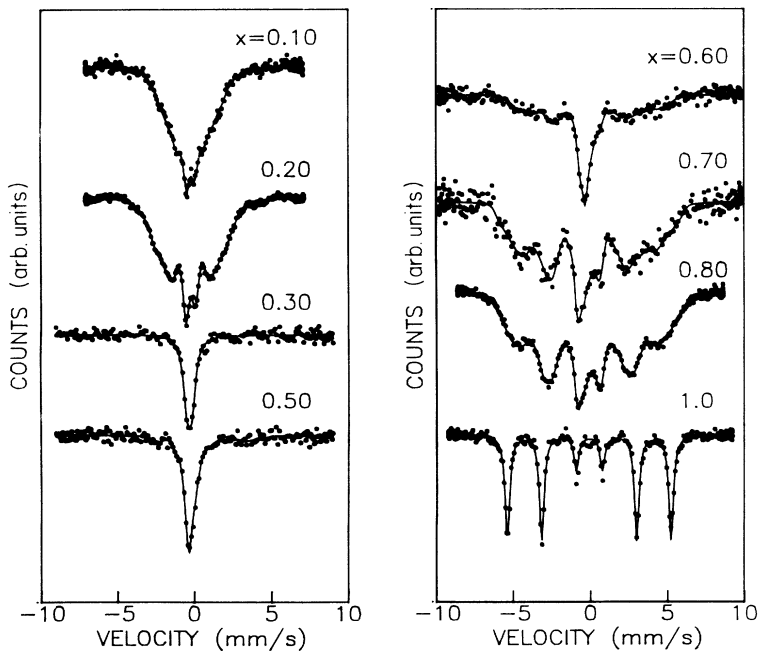

FIG. 2. 4.2-K Mössbauer spectra of the thermal evaporated $Cr_{1-x}Fe_x$ film alloys. The solid lines represent the curves of fitting by a hyperfine field distribution.

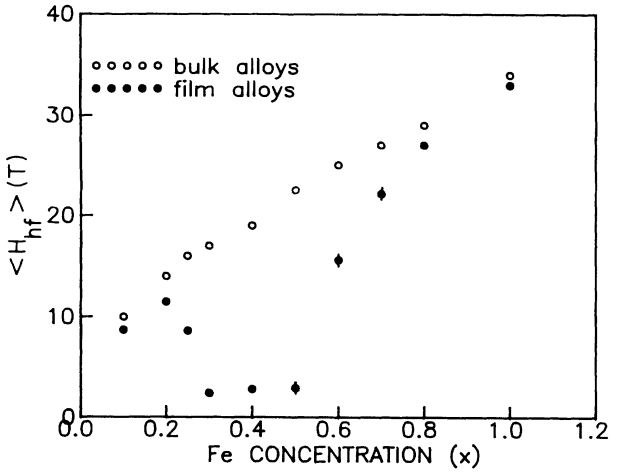

FIG. 3. Concentration dependence of the average hyperfine field, $\langle H_{hf} \rangle$, for $Cr_{1-x}Fe_x$ alloys. (●) the film alloys in the present work and (○) the bulk bcc alloys after Ref. 12.

films with an amorphous structure, the $\langle H_{hf} \rangle$ values are much lower as compared with bulk samples. Since the values of $\langle H_{hf} \rangle$ do not show a pronounced change in the composition range where amorphous phase is prominent, it is still an open question if Fe possesses a magnetic moment (i.e., $\langle H_{hf} \rangle$ may be accidentally zero). Therefore, the broadening of the absorption line may be mainly attributed to the quadrupole interaction.

For the films with $x < 0.6$, The RT Mössbauer spectra exhibit only an absorption line, as shown in Fig. 4, which indicates a paramagnetic character. Due to the quadrupole interaction, the linewidth for the amorphous films ($x = 0.30$ and 0.50) is much broader than that of the crystalline films ($x = 0.10$ and 0.20). The former case was fitted by using a quadrupole splitting distribution (see the inset of Fig. 4), while a singlet was used to fit the latter one where Fe atoms are placed in the chemical environments with a higher symmetry. For $x \geq 0.60$, due to the appearance of the bcc phase with a Curie temperature above RT,[13] the RT Mössbauer spectra are formed by a magnetically split subspectrum overlapping with an absorption line and finally show only the magnetic component for $x \geq 0.8$.

From the positions of the spectra shown in Fig. 4, it can be seen that the average isomer shifts ($\overline{IS}$) of the films with amorphous structure are smaller than those of the films with crystalline structure. The reason may be that, since an amorphous structure is more densely packed than the bcc lattice, there is a higher s electron density at Fe nuclei transferred from Cr whose electronegativity is less than Fe.[11]

The crystallization process of the $Cr_{70}Fe_{30}$ film was followed by *in situ* Mössbauer measurements as shown in Fig. 5. The corresponding annealing temperature dependence of $\overline{IS}$ values are plotted in Fig. 6. For comparison, the $\overline{IS}$ values for a $Cr_{72}Fe_{28}$ bulk crystalline alloy, obtained from the same type of measurements, are also shown in Fig. 6. As one can expect from second-order Doppler shift,[14] the $\overline{IS}$ of the spectra for both samples decreases linearly with the increase of annealing temperature. However, when the amorphous film is heated up to

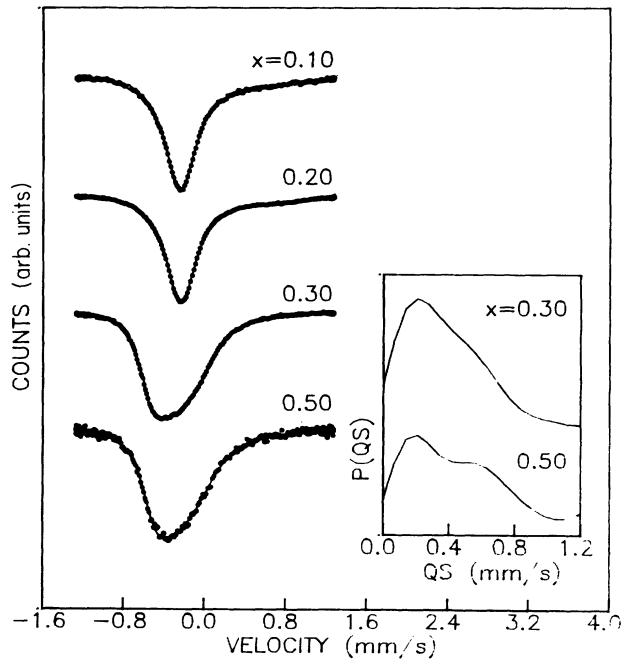

FIG. 4. Room-temperature Mössbauer spectra of the thermal evaporated $Cr_{1-x}Fe_x$ film alloys. The solid lines represent the fits with a singlet for $x = 0.10$ and 0.20 (which have a bcc structure), and with a quadrupole splitting distribution for $x = 0.35$ and 0.50 (which have amorphous structure). The corresponding quadrupole splitting distributions are shown in the inset.

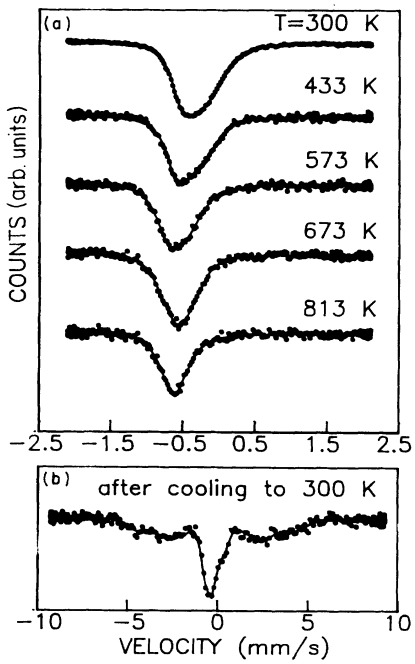

FIG. 5. *In situ* Mössbauer spectra measured in a furnace at the indicated temperatures for the thermal evaporated $Cr_{70}Fe_{30}$ film alloy. (a) the spectra measured as the film was heated up; (b) the room-temperature spectrum measured after the film was cooled down from 540 °C.

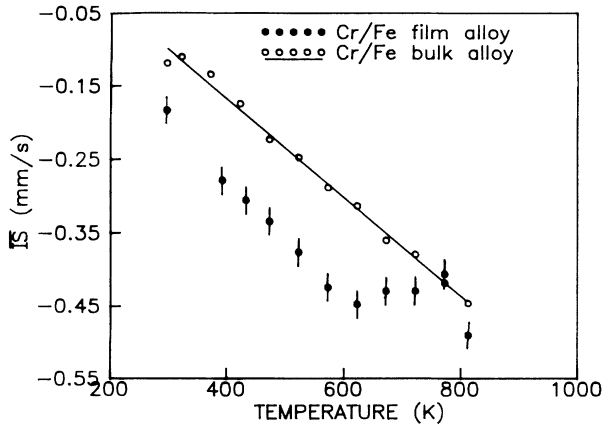

FIG. 6. Temperature dependence of the average isomer shifts, $\overline{\text{IS}}$, obtained from the *in situ* Mössbauer measurements for the thermal evaporated $Cr_{70}Fe_{30}$ film alloy (●) and the $Cr_{72}Fe_{28}$ bulk bcc alloy (○).

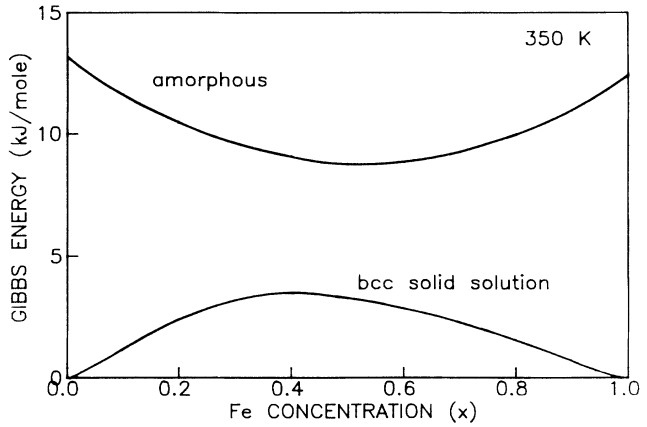

FIG. 7. Calculated Gibbs free-energy diagrams of the amorphous and solid solution states for the Cr-Fe alloy system.

about 630 K, the $\overline{\text{IS}}$ starts to deviate from its linear variation trend and shifts toward the values for the crystalline alloy. Meanwhile, the spectra get narrower (Fig. 5). This is a clear indication of a crystallization process.

It is worth noticing that the crystallization leads to a segregation of two phases, as is reflected in the spectrum at the bottom of Fig. 5. According to the composition dependence of $\langle H_{\text{hf}} \rangle$ (Ref. 12) and IS,[15] the Fe concentration in the two phases can be estimated to be about 50 and 10%, respectively.

IV. DISCUSSION

From the results presented above, one obtains the phase boundaries of amorphous and bcc crystalline phases for the thermal coevaporated $Cr_{1-x}Fe_x$ film alloys. The amorphous single phase is realized for $0.25 < x < 0.60$. The region of coexistence of the two phases was found to be $0.60 \leq x < 0.80$ and $0.20 < x \leq 0.25$. The pure bcc phase is observed for $x \leq 0.20$ and $x \geq 0.80$.

An deeper insight in connection with amorphization mechanism in the $Cr_{1-x}Fe_x$ alloys involves both of the thermodynamics of the system and the kinetics of the condensation process.

In order to evaluate the thermodynamics of the system, Gibbs free-energy diagrams of amorphous and bcc solid solution states for the Cr-Fe system were constructed for the temperature of 350 K as shown in Fig. 7. The values were calculated as follows. The Gibbs free energies, G^0, for pure Fe and Cr metals were taken as 0. The difference in Gibbs free energy between the crystalline and amorphous states, $\Delta G^{a\text{-}c}$, for Fe and Cr metals was estimated from the expression[16]

$$\Delta G^{a\text{-}c}(T) = \frac{\Delta H_f (T_m - T)}{T_m} , \tag{1}$$

where ΔH_f is the heat of fusion, T is the temperature of interest, and T_m is the melting temperature. Then, the Gibbs free energy of amorphous Fe and Cr metals is obtained by $G^a_{\text{Fe}} = \Delta G^{a\text{-}c}_{\text{Fe}} + G^0_{\text{Fe}} = \Delta G^{a\text{-}c}_{\text{Fe}}$ and $G^a_{\text{Cr}} = \Delta G^{a\text{-}c}_{\text{Cr}} + G^0_{\text{Cr}} = \Delta G^{a\text{-}c}_{\text{Cr}}$. The Gibbs free energy of the amorphous Cr-Fe alloys was determined by[7]

$$G^a_{\text{Fe-Cr}} = X_{\text{Fe}} G^a_{\text{Fe}} + X_{\text{Cr}} G^a_{\text{Cr}} + G^a_{\text{mixing}} \tag{2}$$

and

$$G^a_{\text{mixing}} = H^a_{\text{mixing}} - TS^a_{\text{mixing}} ,$$

where the entropy $S^a_{\text{mixing}} = -R(X_{\text{Fe}} \ln X_{\text{Fe}} + X_{\text{Cr}} \ln X_{\text{Cr}})$ is taken assuming an ideal solution and H^a_{mixing}, the enthalpy of mixing, was estimated from Miedema's model adjusted for consideration of chemical short-range order.[17]

The Gibbs free energy for the bcc solid solution was calculated based on one of the latest thermodynamic assessments on the Cr-Fe system proposed by Andersson and Sundman[18] at a temperature of 350 K.

As shown in Fig. 7, the equilibrium state at 350 K shows a miscible gap. However, it had been shown[19] that, under a reasonable fast cooling rate, a high-temperature disordered state will transform to the solid solution (bcc structure), which is the stable phase in a high-temperature range. This is clearly a limitation of the long-range-diffusion kinetics. Since we deal with a problem of vapor condensation, the bcc solid solution is taken as a more stable state in the following discussion.

By comparing the two curves in Fig. 7, it can be seen that the difference in Gibbs free energy, $\Delta G^{a\text{-}c}$, between amorphous and crystalline phases, i.e., the driving force for crystallization, is about 5–6 KJ/mol in the middle of composition range at 350 K. This value is of the order of magnitude of the driving force when crystallization occurs usually at a temperature much higher than 350 K for a typical metallic amorphous. Since the diffusivity of a system increases exponentially with temperature, this comparison may imply that $T = 350$ K would be a too low value for crystallization under such driving force. Namely, an amorphous phase can be maintained in these alloys once it is formed at 350 K. It is also seen from Fig. 7 that the driving force in the two elemental rich sides is much higher. Therefore, from the thermodynamic point of view, the amorphization occurs more easily for films in

a range of composition in the middle [slightly left shifted (see Fig. 7)] than in the two elemental rich sides. This is in agreement with our experimental results.

Now let us consider the condensation process. As mentioned above, a binary alloy system whose constituents have a similar atomic size usually has weaker bonds between different type of atoms (i.e., a smaller heat of mixing, ΔH_{mixing}) in the liquid state. This is also the case for the Cr-Fe system.[20] Therefore, once a Cr-Fe liquid alloy is cooled, which causes the system to deviate from the equilibrium state, the atoms can easily move to a more stable state, i.e., bcc structure by a short-range atomic rearrangement. In the case of vapor quenching, although a quenching rate higher than that of melt quenching can be obtained, such atomic rearrangement from the "hot atoms" which are those just arrived at the substrate may also occur. This may be the reason why Sumiyama, Ohshima, and Nakamura did not obtain amorphous films by sputtering deposition.[11] However, it should be kept in mind that the atomic rearrangement is a cooperatively atomic motion of a group of atoms. The driving force for the rearrangement is the energy difference between the initial and the final states of this group of atoms. Since the deposition rate used in our experiment is very small (25 Å/min), the deposition occurs atom by atom,[21] so that the cooperative rearrangement system may not be well established. Thus, according to Bennett's local model of amorphization, the atoms essentially fall into the energy minimum closest to their arrival points.[22] Taking into account both the thermodynamics of the system and the kinetics of the condensation process, amorphization in Cr-Fe alloys in the middle of the composition range (slightly left shifted) is then more comprehensive. It should also be mentioned that, although a high volume (3×10^{-7} torr) was kept during the depositions, a contamination from residual gases such as O_2 or N_2 may also play some role in stabilizing the amorphous structure.

V. SUMMARY

Although Cr-Fe is not a ready-glass-forming alloy system, we found that, in the middle of the composition range, an amorphous structure can be obtained by thermal evaporation at room temperature by using a very low deposition rate. The low deposition rate may provide a favorable kinetics for amorphization through an atom-by-atom packing, which restricts the occurrence of cooperative interdiffusion from hot atoms. Thus, crystallization resulting from atomic diffusion will be depressed. The calculation of the Gibbs free energy indicates that, once an amorphous phase is formed at a low temperature, the driving forces in the middle of composition range are not strong enough to lead to crystallization. The amorphization in the Cr-Fe system causes a dramatic reduction of the Fe magnetic moment. The isomer shift values are also depressed due to a higher atomically packing density, as compared with the corresponding bcc structure.

ACKNOWLEDGMENTS

We are indebted to Dr. F. C. R. Assunção for his stimulating discussion, G. D. A. Soares for the analysis of the compositions of the films by EDS and R. Abrahao for the x-ray-diffraction measurements. This work was supported by CNPq-SCT Grant No. 500117/90-01.

[1]H. A. David, in *Amorphous Metallic Alloys,* edited by F. E. Lubosky (Butterworth, London, 1983), p. 8.
[2]R. W. Cahn, J. Phys. (Paris) Colloq. **43**, C9-55 (1982).
[3]B. C. Giessen, *Proceedings of the 4th International Conference on Rapidly Quenched Metal* (Japan Institute of Metals, Sendai, 1982), Vol. 1, p. 213.
[4]F. Sommer, Z. Metallkde. **72**, 219 (1981).
[5]*Handbook of Chemistry and Physics,* edited by R. C. Weast, 46th ed. (Chemical Rubber, Boca Raton, 1965), p. 119.
[6]S. K. Xia, E. Baggio-Saitovitch, F. C. R. Assunção, and V. A. P. Rodriguez, J. Phys. Condens. Matter **5**, 2729 (1993).
[7]J. S. C. Jang and C. C. Koch, J. Mater. Res. **5**, 498 (1990).
[8]K. Sumiyama, H. Ezawa, and Y. Nakamura, Phys. Status Solidi A **93**, 81 (1986).
[9]N. Kataoka, K. Sumiyama, and Y. Nakamura, Trans. Jpn. Inst. Met. **27**, 823 (1986).
[10]K. Sumiyama, H. Ezawa, and Y. Nakamura, J. Phys. Chem. Solids **48**, 255 (1987).
[11]K. Sumiyama, N. Ohshima, and Y. Nakamura, Trans. Jpn. Inst. Met. **28**, 699 (1987).
[12]H. Kuwano and K. Ono, J. Phys. Soc. Jpn. **42**, 72 (1977).
[13]S. K. Burke, J. Phys. F **13**, 451 (1983).
[14]R. V. Pound and G. A. Pebka, Phys. Rev. Lett. **4**, 274 (1960).
[15]S. M. Dubiel and G. Inden, Z. Metallkde. **78**, 544 (1987).
[16]D. Turnbull, J. Appl. Phys. **21**, 1122 (1950).
[17]A. W. Weeber, J. Phys. F **17**, 809 (1987).
[18]J. O. Andersson and B. Sundman, CALPHAD **11**, 83 (1987).
[19]W. B. Pearson, *A Handbook of Lattice Spacings and Structures of Metals and Alloys* (Pergamon, New York, 1958), p. 21.
[20]A. K. Niessen, F. R. de Boer, R. Boom, P. F. de Chatel, W. C. M. Mattens, and A. R. Miedema, CALPHAD **7**, 51 (1983).
[21]P. K. Leung and J. G. Wright, Philos. Mag. **30**, 185 (1974).
[22]C. H. Bennett, J. Appl. Phys. **43**, 2727 (1972).